

pubs.acs.org/JPCL Letter

Spatial Patterns of Light-Harvesting Antenna Complex Arrangements Tune the Transfer-to-Trap Efficiency of Excitons in Purple Bacteria

Mykyta Onizhuk, [^] Siddhartha Sohoni, [^] Giulia Galli, and Gregory S. Engel*



Cite This: J. Phys. Chem. Lett. 2021, 12, 6967–6973



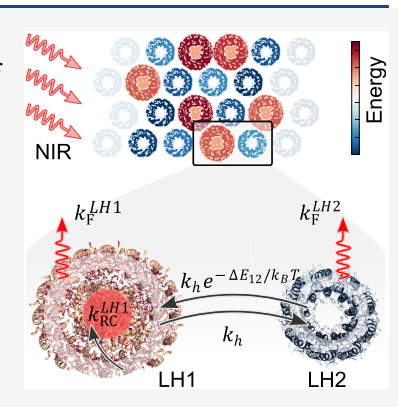
ACCESS

III Metrics & More



Supporting Information

ABSTRACT: In photosynthesis, the efficiency with which a photogenerated exciton reaches the reaction center is dictated by chromophore energies and the arrangement of chromophores in the supercomplex. Here, we explore the interplay between the arrangement of light-harvesting antennae and the efficiency of exciton transport in purple bacterial photosynthesis. Using a Miller—Abrahams-based exciton hopping model, we compare different arrangements of light-harvesting proteins on the intracytoplasmic membrane. We find that arrangements with aggregated LH1s have a higher efficiency than arrangements with randomly distributed LH1s in a wide range of physiological light fluences. This effect is robust to the introduction of defects on the intracytoplasmic membrane. Our result explains the absence of species with aggregated LH1 arrangements in low-light niches and the large increase seen in the expression of LH1 dimer complexes in high fluences. We suggest that the effect seen in our study is an adaptive strategy toward solar light fluence across different purple bacterial species.



hotosynthesis employs a spatio-energetic funnel to maximize the transfer-to-trap efficiency of excitons. 1,2 Chromophores are arranged to absorb from higher to lower energies as they get closer to the reaction center. For example, in cyanobacterial photosynthesis, high-energy excitons created in the phycobilisome move energetically downhill to photosystem I. Within photosystem I, the lowest-energy red chlorophylls spatially surround the RC. 1,3 Another striking example of a spatio-energetic funnel is found in purple bacteria. On purple bacterial intracytoplasmic membranes (ICMs), LH2 proteins absorbing 850 and 800 nm light surround LH1 proteins absorbing light at a longer wavelength (lower energy), 875 nm. Photosynthetic reaction centers (RCs) are embedded in the LH1 proteins, thus creating a well-defined two-step energetic funnel, or downhill hopping gradient for excitons to move from LH2 to LH1 and then on to the RC. 4,5 The funnel facilitates a highly efficient transfer-to-trap process in purple bacteria. The efficiency with which a photogenerated exciton gets quenched at the RC (transfer-to-trap efficiency) has been reported to be in the range of 80-95% for purple bacteria. 1,6-8

Over the past few decades, residue—chromophore interactions that tune the energies of photosynthetic chromophores have been extensively studied.^{3,9–13} On the other hand, the role of the membrane organization in tuning transfer-to-trap efficiency and excitonic pathways is comparatively less explored. In purple bacteria, quinone diffusion, variable internal conversion in RCs, and maximal surrounding of RCs by LH2, among other parameters, have been suggested as drivers of the different arrangements of light-harvesting

complexes observed in nature. 8,14–16 Atomic force microscopy (AFM) studies on purple bacterial ICMs have shown that in *Rb. sphaeroides*, LH1 proteins form dimers and aggregate to make LH1 islands of eight complexes typically arranged in two rows of four (2 × 4), whereas in *Rps. acidophila*, *Rsp. photometricum*, and other species, the distribution of LH1s is random. 5,8,17,18 Light conditions are known to affect LH1:LH2 complex ratios; LH1:LH2 ratios between 1:2 and 1:14, the result of light-dependent LH2 expression, have been reported on purple bacterial ICMs. 19–21 AFM studies have also uncovered a plethora of defects on the lattice structure of the membrane, including LH1s with broken or missing RCs and incorrectly "wrapped" LH2s and LH1s. 17,18,22 Nonphotosynthetic proteins present on the membrane can also disrupt excitonic pathways.

In this work, we examine the effect of different membrane protein arrangements on the robustness and transfer-to-trap efficiency of photosynthesis. We model exciton dynamics with kinetic Monte Carlo simulations based on the Miller—Abrahams model. We verify our model by recovering trends in exciton lifetimes on purple bacterial ICMs with varied LH1:LH2 ratios and light fluences. We find that different

Received: May 13, 2021 Accepted: July 15, 2021 Published: July 20, 2021





arrangements of LH1 and LH2 on the membrane show differences of up to 2% in transfer-to-trap efficiency in the $0.5-100~\mathrm{W/m^2}$ solar fluence regime. We suggest that this difference manifests in an ecological advantage for species with aggregated LH1s over many generations of proliferation and that the formation of LH1 islands is an adaptation strategy to light fluences across purple bacterial species.

The Letter is organized as follows: We begin with describing our adapted computational model of the ICM. We then state the results of our simulations. Finally, we discuss their implications and explain the observed phenomena.

Development of ICM Model. To model exciton dynamics on the purple bacterial ICMs, we use kinetic Monte Carlo exciton hopping simulations incorporating the Miller—Abrahams model of weighting exciton hopping steps on a purple bacterial ICM lattice. This model is naturally dissipative, and downhill hopping of excitons is favored over uphill hopping. Specifically, downhill hops between a donor, i, and an acceptor, j, proceed with a fixed rate constant $k_{\rm h}$, but uphill hops are weighted by the Boltzmann factor of the energy difference ΔE_{ij} between the two chromophores i and j:

$$k_{ij} = k_h \exp \left[-\left(\frac{\Delta E_{ij} + |\Delta E_{ij}|}{2k_B T} \right) \right]$$
 (1)

Here, k_{ii} is the hopping rate between i and j. $k_{\rm B}$ is the Boltzmann constant, and T is the temperature. We assume that the rates of LH1 and LH2 fluorescence and transfer of excitons to the RC are constant. The Miller-Abrahams model has been used previously to describe spin-hopping on lattices, exciton hopping in nanoparticle arrays, and charge hopping in organic photovoltaics. 24-26 Because of its preferential downhill hopping feature which mirrors the energetic funnel in photosynthesis, Miller-Abrahams weighting of hopping steps is particularly suitable for exciton simulations on purple bacterial ICMs. Other models including FRET can incorporate downhill funneling, static disorder, 27 and distance dependence in simulations. However, when many like complexes are involved and the intercomplex distance is fixed because of a lattice structure, the Miller-Abrahams model can be used to recover salient features of incoherent hopping if the relevant hopping constants are known experimentally.

The purple bacterial ICM is modeled by a 24×24 periodic two-dimensional hexagonal lattice; each lattice site is occupied by either an LH1 or LH2 protein. 16,17 We use a hexagonal lattice as an approximation to structures reported in multiple AFM studies showing prominent hexagonal close packing of proteins.^{8,16} Each site is assigned an energy randomly picked from a Gaussian energy distribution with widths obtained from the measured fluorescence line widths of LH1 and LH2 $(10930.5 \pm 119.5 \text{ cm}^{-1} \text{ for LH1 and } 11547 \pm 72 \text{ cm}^{-1} \text{ for}$ LH2). 28-30 For the 1:2 ratio lattice, the exciton is created at a random position on the lattice, with a 14% chance of being created on LH1 and otherwise on LH2, in accordance with the absorption cross section at 800 nm. 19 For all other ratios, we have interpolated the exciton branching ratios obtained by Timpmann and co-workers¹⁹ for our model. These ratios are tabulated in Supporting Table 1. The intercomplex hopping rate from lattice site i to j is determined by eq 1. Temperature is set to 298 K for all simulations. The hop constant k_h in eq 1 is set to the experimentally measured value of 0.06173 ps The rate of fluorescence is assumed to be constant for each type of protein and is consistent with experimentally measured

fluorescence lifetimes of the corresponding complexes: $k_{\rm F}^{\rm LH1} = 0.005~{\rm ps^{-1}}^{31}$ and $k_{\rm F}^{\rm LH2} = 0.0025~{\rm ps^{-1}}^{.32}$ The only free parameter left is the transfer rate from LH1 to the RC, which is obtained as $k_{\rm RC}^{\rm LH1} = 0.015625~{\rm ps^{-1}}$ by fitting the exciton lifetime in the membrane with an LH1:LH2 ratio of 1:2 to 60 ps. ¹⁹ Hops beyond nearest neighbors are neglected owing to the strong distance dependence of incoherent hopping.

To compute exciton lifetime as a function of LH2 expression, we use LH1:LH2 ratios of 1:2, 1:3, 1:4, 1:5, and 1:6 with random arrangements of LH1 and LH2 on the membrane. In this work, we also seek to explore the robustness of this light-harvesting system against the placement of nonphotosynthetic proteins on the ICM and gaps introduced because of the curvature of the membrane. To do so, we model a defect site on the membrane as a lattice site with effectively infinite energy, i.e., a void to which an exciton cannot hop. In the real system, this "defect" is likely a membrane protein other than LH2 or LH1. We keep the LH1:LH2 ratio constant at 1:2 and vary the fraction of defective sites on the membrane. LH1, LH2, and defect placements are random.

To examine the effect of LH1 arrangements on transfer-to-trap efficiency at all physical fluences, in our simulations we account for the difference between the photon absorption rate and the rate of exciton dissociation at the RC (RC turnover rate) using a dynamic RC closing method.⁴ Across much of the physiological solar fluence range the photon absorption rate of the membrane is greater than the RC turnover rate, creating a bottleneck for exciton quenching.

Solar fluence in typical purple bacterial environmental niches can range from 0.1 to 1000 W/m^2 , which corresponds to peak sunlight fluence at the equator. At the low end, photon absorption on our simulated membrane and physiological membranes occurs once in every 10 ms, while in the highfluence limit, a photon is absorbed approximately once every 1 μ s.⁴ Even in the highest solar fluence, multiexciton events are rare on purple bacterial ICMs because the exciton lifetime is maximally 200 ps—orders of magnitude smaller than the photon absorption rate. Therefore, we investigate lifetime and number of exciton hops as a function of light fluence within the single exciton regime. However, if the quinone release step of the exciton quenching process step (1-100 ms time scale for one exciton) is slower than the photon absorption rate, an incoming exciton cannot hop to an exciton dissociating RC to be quenched. This phenomenon is called RC blocking in our work, and it determines exciton lifetimes in the high-fluence limit. We include RC blocking in our model by adopting a strategy similar to that of Fassioli et al.4 RCs are blocked (transfer to RC is turned off) for a variable number of subsequent simulations after the RC traps an exciton. This number is denoted by N_{block} . The relationship between light fluence and number of subsequent blocked simulations depends on the membrane absorption cross section and the exact turnover time of the RC and is given by

$$N_{\text{block}} = \frac{I\sigma\lambda}{hc} \frac{1}{r} = \frac{N_{\text{photons}}}{r} \tag{2}$$

where h is Planck's constant, λ the incident wavelength (800 nm), I the light fluence, r the RC turnover rate, σ the membrane absorption cross section, c the speed of light, and $N_{\rm photons}$ the number of photons absorbed by the membrane per unit time. RC turnover times were not measured in previous fluence-dependent exciton lifetime studies on purple bacterial ICMs^{19,33} and are not known for the samples used in these

studies. NaCl concentration, pH, and quinone availability have been shown to affect RC turnover rates, and the turnover times in laboratory conditions for the samples used in the two previous studies could be different by an order of magnitude. 34,35 In this study, we use an RC turnover time of 25 ms/exciton, consistent with previous independent experimental and theoretical works across different species. 4,54,35 The ratio of the number of photons absorbed per second and the RC turnover rate yields $N_{\rm block}$. In our approach, we first calculate the full membrane absorption cross section using the molar absorption coefficients of bacteriochlorophylls B800 and B850 in LH2 of 226 and 2.5 mM⁻¹ cm⁻¹, respectively, ³⁶ at 800 nm and a partition ratio of 14:86¹⁹ of excitons between LH1 and LH2. The membrane contains LH1s and LH2s in 1:2 ratios, and 14 excitons are created on each LH1 for every 86 excitons created on each LH2. The partition ratios of excitons used for other LH1:LH2 ratios are tabulated in Supporting Table 2 and are adapted from Timpmann et al. 19 (Supporting Table 1). From these values, we calculate that 1.4×10^{5} photons are absorbed per second at a 100 W/m² light fluence by our 24×24 hexagonal membrane.

To investigate if the supercomplex structure affects transferto-trap efficiency, we construct three lattice structures ("random", "island" with groups of LH1s clustered together, and "isolated" with all LH1s separated by LH2s) for further fluence-dependent Monte Carlo exciton dynamics simulations. The first lattice is a random arrangement of LH1s and LH2s in the 1:2 ratio, which represents the high-light membranes of bacteria such as Rsp. photometricum and Rps. acidophila. Simulations for this structure are performed on 144 different random arrangements to obtain the data shown in this work. The second lattice consists of 2 × 4 LH1 islands surrounded by LH2 such that the LH1:LH2 ratio is 1:2. This arrangement represents many species in the Rhodobacter genus. The third is an idealized "isolated" lattice of a two-dimensional hexagonal AB₂ arrangement that eliminates adjacent LH1 neighbors. Data collected on different ratios, defects, and light fluences is averaged over 72 000 000 exciton trajectories across 144 spatial and energetic realizations of the membranes. We assume that membrane curvature does not strongly change exciton dynamics.^{37–42} We note that while we assume the hopping rate, $k_{\rm b}$ to be constant, it has been shown that intercomplex distance changes because of membrane curvature and the average hopping time between two LH2 complexes can range between 4 and 25 ps because of different intercomplex distances. Finally, we assume that the ~ 150 cm⁻¹ static disorder of LH complexes rules out resonance enhancement of Forster hopping for certain energy differences in accordance with earlier work by Jang⁴³ and Schulten⁴⁴ and co-workers.

Observations from Simulations. First, we look at the effect of LH1:LH2 ratios on exciton dynamics. Exciton lifetimes from our simulations, as shown in Figure 1A, are in good agreement with earlier experimentally determined lifetimes for the different ratios of LH1 and LH2 expression. An earlier theoretical work calculated a 50 ps lifetime for a 1:2.8 LH1:LH2 ratio. As the LH1:LH2 ratio increases from 1:2 to 1:6, the exciton lifetime increases from ~60 to 82 ps (Figure 1A). Our simulations also show that the increasing LH1:LH2 ratio leads to an increase in fluorescence quantum yield, or lower transfer-to-trap efficiency (Figure 1B). Looking at the constituent hops of the average exciton trajectory, we find that only hops between LH2s increase significantly (Figure 1C) as a function of LH2 expression and LH1 to LH1 hops decrease

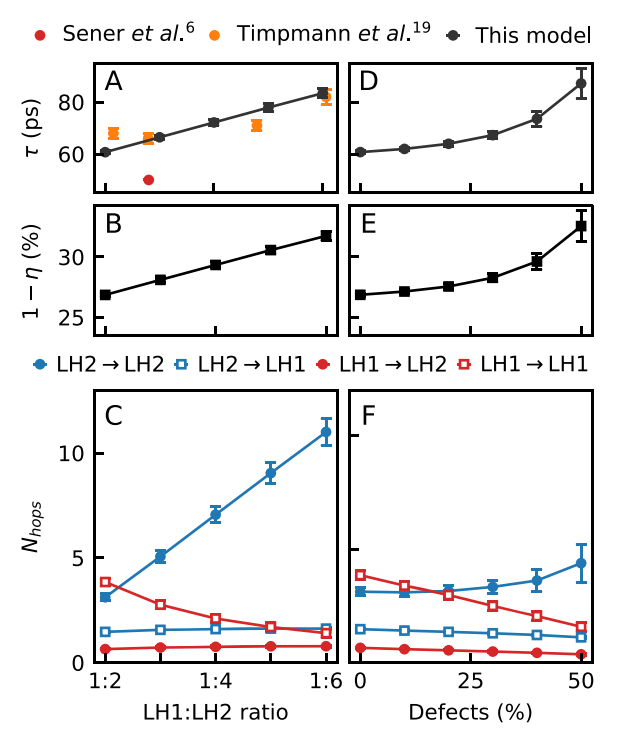


Figure 1. (A) Trend of exciton lifetimes (τ) from our model plotted against experimentally obtained lifetimes by Timpmann $et~al.^{19}$ and the theoretically calculated lifetime by Sener $et~al.^{6}$ for different LH1:LH2 ratios. (B) Trend of fluorescence quantum yield $(1-\eta)$ values obtained from our simulations for different LH1:LH2 ratios. (C) Number of hops from LH2 to LH2, LH2 to LH1, LH1 to LH2, and LH1 to LH1 as a function of LH1:LH2 ratio. (D) Trend of exciton lifetimes (τ) as a function of percentage of defect sites on the membrane lattice. (E) Trend of quantum yield values as a function of percentage of defect sites. (F) Number of hops from LH2 to LH2, LH2 to LH1, LH1 to LH2, and LH1 to LH1. Error bars correspond to one population standard deviation (1SD).

concomitantly. Irrespective of the LH1:LH2 ratio, exciton hopping from LH2 to LH1 and back-hopping from LH1 to LH2 do not change significantly (on average 1.46 to 1.62 times and 0.65 to 0.78 times, respectively, over an exciton's lifetime).

Our simulations show that exciton lifetime increases with the percentage of defective lattice sites (Figure 1D). For up to 30% defective sites, the transfer-to-trap efficiency of the membrane decreases by only ~2% (Figure 1E), after which it decreases more sharply. Looking at the types of exciton hops, we see that only hops between LH2s increase (Figure 1F). Hops between LH1 decrease appreciably and hops from LH1 to LH2 and LH2 to LH1 show a small decrease with increasing percentage of defects.

We recover the experimentally observed trend of exciton lifetime as a function of light fluence. 19,33 Using an RC turnover rate of 25 ms/exciton, 4,34,35 we find particularly good agreement with the experimental work of Borisov *et al.* 33 A saturation limit lifetime of 200 ps is obtained for the single-exciton regime in accordance with our chosen LH1 fluorescence lifetime (Figure 2A). A small increase is seen in hops between LH2s, from LH1 to LH2, and from LH2 to LH1. The largest increase is seen in inter-LH1 hops as a function of $N_{\rm block}$ (from ~4 to 16 hops, Figure 2B). Figure 2C shows representative exciton trajectories on the lattice under low light ($N_{\rm block}=0$) and high light ($N_{\rm block}=10\,000$) conditions. We see that in high light, the sampling region of

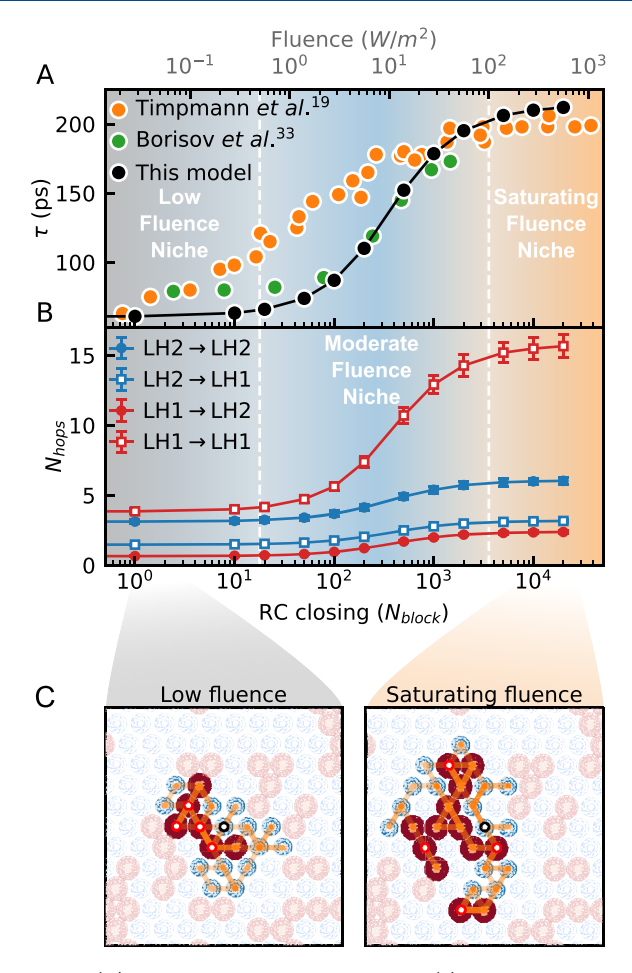


Figure 2. (A) Trend of fluorescence lifetimes (τ) obtained from our simulations as a function of RC closing and light fluence plotted with experimentally measured lifetimes as a function of light fluence by Timpmann *et al.*¹⁹ and Borisov *et al.*³³ (B) Number of hops as a function of subsequent RC blocking iterations. (C) Four sample trajectories for RC closing $(N_{\rm block})$ values of 0 and 10 000. Trajectories start at the LH2 with a black outline circle and end at the circles with red outlines. Brightness of yellow lines indicates the number of hops between two pairs of complexes and highlights the increased inter-LH1 hops. Mean lifetime is preserved while randomly picking trajectories to represent. LH1, red; LH2, blue. Error bars show 1SD.

the exciton increases (Supporting Figure 1), and there is a greater number of inter-LH1 hops.

Fluence-dependent Monte Carlo simulations on the random, isolated, and island arrangements (Figure 3A) reveal that the transfer-to-trap efficiency of each of the three lattice structures follows the same qualitative trend as a function of RC blocking (Supporting Figure 2). However, differences in transfer-to-trap efficiency are observed when we consider the deviation of the three efficiency curves from average for each fluence range (Figure 3B). At saturating fluences (≥100 W/ m^2 ; $N_{block} \ge 3000$), all arrangements have the same efficiency. At low fluences (corresponding to negligible RC blocking), the isolated LH1 structure is ~1% more efficient than the random and island structures. Strikingly, at $N_{\rm block}$ values between 20 and 3000, the island LH2 arrangement is the most efficient, outperforming the random and isolated structures by \sim 1% and ~2%, respectively. This effect persists when 20% defects are added to all three arrangements while keeping the ratio between LH1 and LH2 constant (Figure 3C), but it is not seen

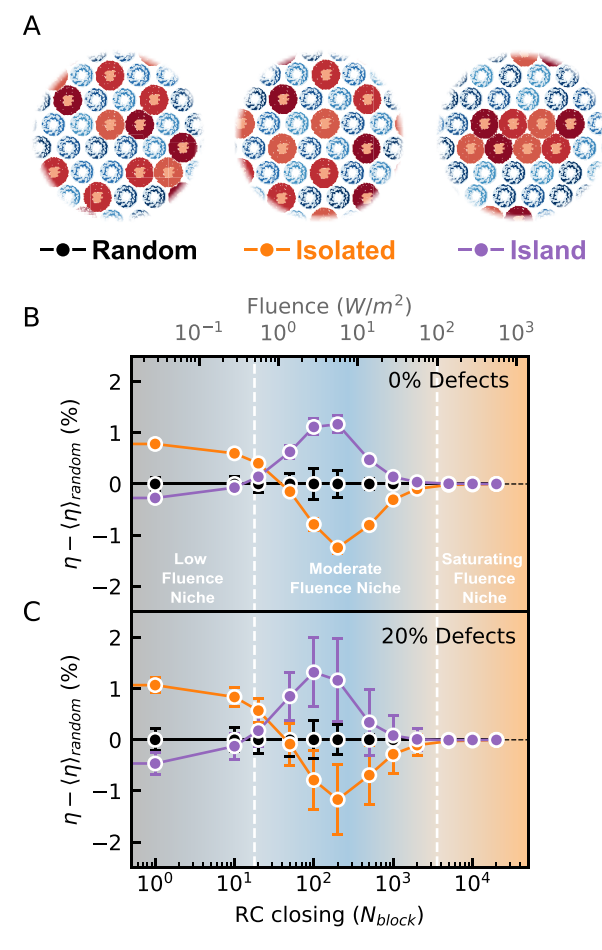


Figure 3. (A) Representative sections of random, isolated, and island lattice structures. LH1s and LH2s are randomly distributed in a 1:2 ratio in the random lattice; isolated and island structures are repeated over the 24 \times 24 membrane. (B) Random, island, and isolated structure efficiency deviations from the average random efficiency $\langle \eta \rangle_{\rm random}$ as a function of $N_{\rm block}$ for a lattice without defects. (C) Random, island, and isolated structure efficiency deviations from the average random efficiency $\langle \eta \rangle_{\rm random}$ as a function of $N_{\rm block}$ for a lattice with 20% defects. Error bars show 1SD.

when static disorder is increased artificially to twice or four times the physiological disorder (Supporting Figures 3–5). Exciton lifetimes do not change significantly between arrangements in the low- and high-fluence limits, with the isolated structure lifetime being smaller by 3–4 ps (Supporting Table 3). We find that the exciton travels farther from its origin in the island and random arrangements than in the isolated arrangement and that the diffusivity of the island arrangement decays most rapidly in all light fluences (Supporting Figure 6). We also find that difference in efficiency persists when the hopping rate between complexes, $k_{\rm h}$, is increased (Supporting Figure 7) or the LH1:LH2 ratio is changed to 1:5 (Supporting Figure 8).

Discussion of Observations. We first look at the impact of LH1:LH2 ratios on exciton dynamics. The remarkable robustness of the energy funnel in purple bacteria is underlined by the stable rate of back-hopping from the low-energy LH1 pools to high-energy LH2s, even with high LH2 expression. Our observation that only inter-LH2 hops increase substantially for high LH2 ratios is consistent with earlier work showing that increased LH2 expression is not associated with enhanced exciton transfer from LH2 to LH1²⁰ (Figure 1C). In

the case of defects, up to 30% defects have only small effects on the different constituent hops, underlining the robustness of the ICM structure. In our simulations, we only model defects as sites to which the exciton cannot hop, but defective placement of bacteriochlorophylls can lead to LH1s or LH2s with very different energies or exciton hopping rates. We do not incorporate the effect of these defects into our simulations.

In our study of the effect of fluence on transfer-to-trap efficiency, we observe a large increase in inter-LH1 hops in simulations of high RC blocking. This increase indicates that even in high light fluences—when most RCs are closed to incoming excitons-LH2s are effectively excluded from the diffusion region to maximize the probability of the exciton finding an open RC (Supporting Figure 1). This effect is clearly seen in Figure 2C, where sample trajectories show that LH1s are sampled far more than LH2s in high light. It is worth noting that our a priori chosen RC turnover rate of 25 ms/ exciton from Fassioli et al., 4 consistent with other experimental measurements, 33,34 yields good agreement with fluencedependent lifetimes from the experimental work of Borisov et al.33 shown in Figure 2A. We further obtain a best fit RC turnover rate of 22.7 ms/exciton for the study by Borisov et al.33 and a best fit RC turnover rate of 143 ms/exciton for the study by Timpmann et al.¹⁹ It is likely that different RC turnover rates in laboratory conditions among other factors could have led to differences in the fluence dependence of lifetimes measured by Borisov et al.³³ and Timpmann et al.

Previous studies have suggested that quinone release, and not uptake, is the rate-limiting step in the RC turnover making the physiological RC turnover of random (*P. molischianum*)⁴⁶ and island (*Rb. sphaeroides*)⁴⁷ comparable at 25 ms/exciton. At comparable RC turnover rates, the island arrangement could provide *Rb. sphaeroides* with a transfer-to-trap efficiency advantage over other random structures. It should be noted that pH and NaCl ionic strength strongly impact the RC turnover rate^{34,35,48} in experimental conditions and a fluctuating RC turnover rate in turn impacts transfer-to-trap efficiency. Thus, our comparison of the two structures' transfer-to-trap efficiency as a function of light fluence is restricted to the case in which RC turnover rates are the same.

Efficiency differences between the island, random, and isolated arrangements (Figure 3) shed light on the effect of spatial arrangement on transfer-to-trap efficiencies in different light conditions. In the saturation limit, the three membranes show transfer-to-trap efficiency approaching 0% as all RCs are closed and almost all excitons fluoresce. The higher photosynthetic efficiency of the isolated structure at low fluence is likely due to maximal encircling of every LH1 by LH2s, offering a possible one-hop pathway for excitons to reach an open LH1-embedded RC. These results are consistent with an earlier study⁸ in which a similar "isolated"-type structure was found to be more efficient for transfer-to-trap under low-light conditions than other structures. However, upon taking solar fluences into account, a single structure is not the clear winner in terms of transfer-to-trap efficiency. At the typical niche fluences between 0.5 and 100 W/m², the island structure shows an enhanced transfer-to-trap efficiency by \sim 1%. Thus, if RC turnover rates are similar in random and island structures found in nature and limited by quinone release, the island structure could provide an efficiency advantage over the random arrangement.

The replication of this trend with 20% defects and with faster hopping rates (Supporting Figure 7) suggests that this

effect is robust to the placement of nonlight harvesting proteins like cytochromes, defective proteins, and gaps induced because of the curvature of the membrane vesicle. An earlier work on Photosystem I showed a similar robustness of the protein to chlorophyll *a* deletion, where the photosynthetic efficiency of the reaction center was not affected by more than 3% upon the random deletion of any chlorophyll molecule outside of the reaction center. 49

Our finding that the isolated LH1 arrangement performs better in low light is consistent with published membrane AFM images of species inhabiting low-light environments. Isolated LH1 complexes are clearly seen in the "random"-type arrangements found in these species. For example, *Roseobacter* species that inhabit temperate polar oceans and likely experience low light manifest prominent unconnected monomeric LH1 structures in AFM images; ^{50,51} species observed in Antarctic seas at depths substantially below the depth at which only 1% of the surface light reaches show the presence of isolated LH1s. ^{52–55}

On the other hand, according to our findings, the formation of LH1 islands is deleterious to transfer-to-trap efficiency in low-light environments. In nature, while species with random arrangements (e.g., *Rhodopseudomonas* genus) exist in niches with low, moderate, and high solar fluences, species with prominent LH1 island arrangements, such as *Rhodobacter*, have been found only in medium- and high-fluence niches. For the 1:5 LH1:LH2 ratio, the island structure still outperforms the random and isolated structured membranes (Supporting Figure 8), but the difference is small in the medium-fluence regime. At low fluences, however, a sharp drop in transfer-to-trap efficiency is seen for the island structure. This finding combined with the fact that LH2 expression is much higher than LH1 expression in low-light growth, explains why island arrangements are found in medium- and high-fluence niches only.

Further, within *Rb. sphaeroides*, the expression of RC-LH1-PufX dimers that form LH1 islands has been shown to increase drastically in high light intensity growth⁵⁶ and suggests that LH1 island formation is indeed light fluence driven. However, AFM images of low-light grown *Rb. sphaeroides* from a different study do not show a significant presence of monomeric LH1s.⁵⁷ It is likely that the adaptive strategy we suggest manifests across different species. Therefore, we hypothesize that the remarkable 1% enhanced efficiency of the island arrangement (compared to the random arrangement) across a wide range of physiologically relevant light fluences (0.5 to 100 W/m²) provides species of the *Rhodobacter* genus with a significant competitive advantage in well-lit environments. An extensive AFM-based comparison between species will be needed to completely validate our hypothesis.

In summary, our study uses Miller—Abrahams weighting of exciton hopping on purple bacterial intracytoplasmic membranes to show that the formation of LH1 2 × 4 islands increases the transfer-to-trap efficiency of photosynthesis in moderate- to high-light environments while random arrangements work well in low-fluence environments. Our result explains the notable absence of species with aggregated LH1 structures in low-light habitat and the drastic increase seen in the expression of dimeric LH1 complexes by Jones and coworkers. This effect is robust against gaps induced by photosynthetic membrane curvature and the presence of nonphotosynthetic proteins. We believe that the effect could be harnessed in future artificial photosynthesis design efforts

because redox and electrochemistry are typically slower than exciton transport in materials. ^{1,10}

ASSOCIATED CONTENT

Supporting Information

The Supporting Information is available free of charge at https://pubs.acs.org/doi/10.1021/acs.jpclett.1c01537.

Additional figures and tables as described in the text; additional discussion of exciton diffusivity, the role of static disorder, and sources of data (PDF)

AUTHOR INFORMATION

Corresponding Author

Gregory S. Engel – Department of Chemistry, James Franck Institute, and The Institute for Biophysical Dynamics, The University of Chicago, Chicago, Illinois 60637, United States; © orcid.org/0000-0002-6740-5243;

Email: gsengel@uchicago.edu

Authors

Mykyta Onizhuk – Department of Chemistry, The University of Chicago, Chicago, Illinois 60637, United States

Siddhartha Sohoni – Department of Chemistry, James Franck Institute, and The Institute for Biophysical Dynamics, The University of Chicago, Chicago, Illinois 60637, United States

Giulia Galli – Department of Chemistry and Pritzker School of Molecular Engineering, The University of Chicago, Chicago, Illinois 60637, United States; Materials Science Division and Center for Molecular Engineering, Argonne National Laboratory, Lemont, Illinois 60439, United States;

orcid.org/0000-0002-8001-5290

Complete contact information is available at: https://pubs.acs.org/10.1021/acs.jpclett.1c01537

Author Contributions

[∆]M.O. and S.S. contributed equally to this work.

Notes

The authors declare no competing financial interest.

ACKNOWLEDGMENTS

This work was supported by the Air Force Office of Scientific Research (AFOSR) (FA9550-18-1-0099) and the DOE Office of Science (under Award No. DE-SC0020131). The NSF (under Grant No. 1900359) partially supported S.S. to work on ultrafast models of energy transfer dynamics. This work was completed in part with resources provided by the University of Chicago's Research Computing Center and received support from the University of Chicago Materials Research Science and Engineering Center, which is funded by the NSF (under Grant Nos. DMR-1420709 and DMR-2011854). The authors thank Dr. Karen M. Watters for scientific editing and Dr. Marco A. Allodi and Mr. Colin R. Scheibner for helpful discussions.

REFERENCES

- (1) Blankenship, R. Molecular Mechanisms of Photosynthesis, 2nd ed.; Wiley Blackwell: Oxford, U.K., 2014.
- (2) Scholes, G. D.; Fleming, G. R.; Olaya-Castro, A.; van Grondelle, R. Lessons from Nature about Solar Light Harvesting. *Nat. Chem.* **2011**, 3 (10), 763–774.
- (3) Lee, Y.; Gorka, M.; Golbeck, J. H.; Anna, J. M. Ultrafast Energy Transfer Involving the Red Chlorophylls of Cyanobacterial Photo-

- system I Probed through Two-Dimensional Electronic Spectroscopy. J. Am. Chem. Soc. 2018, 140 (37), 11631–11638.
- (4) Fassioli, F.; Olaya-Castro, A.; Scheuring, S.; Sturgis, J. N.; Johnson, N. F. Energy Transfer in Light-Adapted Photosynthetic Membranes: From Active to Saturated Photosynthesis. *Biophys. J.* **2009**, *97* (9), 2464–2473.
- (5) Dahlberg, P. D.; Ting, P.-C.; Massey, S. C.; Allodi, M. A.; Martin, E. C.; Hunter, C. N.; Engel, G. S. Mapping the Ultrafast Flow of Harvested Solar Energy in Living Photosynthetic Cells. *Nat. Commun.* **2017**, *8* (1), 988.
- (6) Sener, M. K.; Olsen, J. D.; Hunter, C. N.; Schulten, K. Atomic-Level Structural and Functional Model of a Bacterial Photosynthetic Membrane Vesicle. *Proc. Natl. Acad. Sci. U. S. A.* **2007**, *104* (40), 15723–15728.
- (7) Ritz, T.; Park, S.; Schulten, K. Kinetics of Excitation Migration and Trapping in the Photosynthetic Unit of Purple Bacteria. *J. Phys. Chem. B* **2001**, *105* (34), 8259–8267.
- (8) Sturgis, J. N.; Niederman, R. A. Atomic Force Microscopy Reveals Multiple Patterns of Antenna Organization in Purple Bacteria: Implications for Energy Transduction Mechanisms and Membrane Modeling. *Photosynth. Res.* **2008**, *95* (2–3), *269*–278.
- (9) Sohail, S. H.; Dahlberg, P. D.; Allodi, M. A.; Massey, S. C.; Ting, P.-C.; Martin, E. C.; Hunter, C. N.; Engel, G. S. Communication: Broad Manifold of Excitonic States in Light-Harvesting Complex 1 Promotes Efficient Unidirectional Energy Transfer *in vivo. J. Chem. Phys.* 2017, 147 (13), 131101.
- (10) Proppe, A. H.; Li, Y. C.; Aspuru-Guzik, A.; Berlinguette, C. P.; Chang, C. J.; Cogdell, R.; Doyle, A. G.; Flick, J.; Gabor, N. M.; van Grondelle, R.; et al. Bioinspiration in Light Harvesting and Catalysis. *Nat. Rev. Mater.* **2020**, *5* (11), 828–846.
- (11) Cogdell, R. J.; Gall, A.; Köhler, J. The Architecture and Function of the Light-Harvesting Apparatus of Purple Bacteria: From Single Molecules to *in vivo* Membranes. *Q. Rev. Biophys.* **2006**, 39 (3), 227–324.
- (12) Wu, J.; Liu, F.; Shen, Y.; Cao, J.; Silbey, R. J. Efficient Energy Transfer in Light-Harvesting Systems, I: Optimal Temperature, Reorganization Energy and Spatial—Temporal Correlations. *New J. Phys.* **2010**, *12* (10), 105012.
- (13) Gellings, E.; Cogdell, R. J.; van Hulst, N. F. Room-Temperature Excitation—Emission Spectra of Single LH2 Complexes Show Remarkably Little Variation. *J. Phys. Chem. Lett.* **2020**, *11* (7), 2430—2435.
- (14) Caycedo-Soler, F.; Rodríguez, F. J.; Quiroga, L.; Johnson, N. F. Interplay between Excitation Kinetics and Reaction-Center Dynamics in Purple Bacteria. *New J. Phys.* **2010**, *12* (9), No. 095008.
- (15) Caycedo-Soler, F.; Rodríguez, F. J.; Quiroga, L.; Johnson, N. F. Light-Harvesting Mechanism of Bacteria Exploits a Critical Interplay between the Dynamics of Transport and Trapping. *Phys. Rev. Lett.* **2010**, *104* (15), 158302.
- (16) Sundström, V.; Pullerits, T.; van Grondelle, R. Photosynthetic Light-Harvesting: Reconciling Dynamics and Structure of Purple Bacterial LH2 Reveals Function of Photosynthetic Unit. *J. Phys. Chem. B* **1999**, *103* (13), 2327–2346.
- (17) Bahatyrova, S.; Frese, R. N.; Siebert, C. A.; Olsen, J. D.; van der Werf, K. O.; van Grondelle, R.; Niederman, R. A.; Bullough, P. A.; Otto, C.; Hunter, C. N. The Native Architecture of a Photosynthetic Membrane. *Nature* **2004**, *430* (7003), 1058–1062.
- (18) Scheuring, S.; Reiss-Husson, F.; Engel, A.; Rigaud, J.-L.; Ranck, J.-L. High-Resolution AFM Topographs of *Rubrivivax gelatinosus* Light-Harvesting Complex LH2. *EMBO J.* **2001**, 20 (12), 3029–3035.
- (19) Timpmann, K.; Chenchiliyan, M.; Jalviste, E.; Timney, J. A.; Hunter, C. N.; Freiberg, A. Efficiency of Light Harvesting in a Photosynthetic Bacterium Adapted to Different Levels of Light. *Biochim. Biophys. Acta, Bioenerg.* **2014**, *1837* (10), 1835–1846.
- (20) Driscoll, B.; Lunceford, C.; Lin, S.; Woronowicz, K.; Niederman, R. A.; Woodbury, N. W. Energy Transfer Properties of *Rhodobacter sphaeroides* Chromatophores during Adaptation to Low Light Intensity. *Phys. Chem. Chem. Phys.* **2014**, *16* (32), 17133–17141.

- (21) Scheuring, S.; Rigaud, J.-L.; Sturgis, J. N. Variable LH2 Stoichiometry and Core Clustering in Native Membranes of Rhodospirillum photometricum. EMBO J. 2004, 23 (21), 4127–4133.
- (22) Olsen, J. D.; Adams, P. G.; Jackson, P. J.; Dickman, M. J.; Qian, P.; Hunter, C. N. Aberrant Assembly Complexes of the Reaction Center Light-Harvesting 1 PufX (RC-LH1-PufX) Core Complex of Rhodobacter sphaeroides Imaged by Atomic Force Microscopy. J. Biol. Chem. 2014, 289 (43), 29927–29936.
- (23) Miller, A.; Abrahams, E. Impurity Conduction at Low Concentrations. *Phys. Rev.* **1960**, *120* (3), 745–755.
- (24) Li, H.; Sini, G.; Sit, J.; Moulé, A. J.; Bredas, J.-L. Understanding Charge Transport in Donor/Acceptor Blends from Large-Scale Device Simulations Based on Experimental Film Morphologies. *Energy Environ. Sci.* **2020**, *13* (2), 601–615.
- (25) Singh, R.; Kim, M.; Lee, J.-J.; Ye, T.; Keivanidis, P. E.; Cho, K. Excimer Formation Effects and Trap-Assisted Charge Recombination Loss Channels in Organic Solar Cells of Perylene Diimide Dimer Acceptors. J. Mater. Chem. C 2020, 8 (5), 1686–1696.
- (26) Gilmore, R. H.; Winslow, S. W.; Lee, E. M. Y.; Ashner, M. N.; Yager, K. G.; Willard, A. P.; Tisdale, W. A. Inverse Temperature Dependence of Charge Carrier Hopping in Quantum Dot Solids. *ACS Nano* **2018**, *12* (8), 7741–7749.
- (27) Lee, E. M. Y.; Tisdale, W. A.; Willard, A. P. Can Disorder Enhance Incoherent Exciton Diffusion? *J. Phys. Chem. B* **2015**, *119* (30), 9501–9509.
- (28) Rutkauskas, D.; Novoderezkhin, V.; Cogdell, R. J.; van Grondelle, R. Fluorescence Spectral Fluctuations of Single LH2 Complexes from *Rhodopseudomonas acidophila* Strain 10050 †. *Biochemistry* **2004**, *43* (15), 4431–4438.
- (29) Schlau-Cohen, G. S.; Wang, Q.; Southall, J.; Cogdell, R. J.; Moerner, W. E. Single-Molecule Spectroscopy Reveals Photosynthetic LH2 Complexes Switch between Emissive States. *Proc. Natl. Acad. Sci. U. S. A.* **2013**, *110* (27), 10899–10903.
- (30) Law, C. J.; Cogdell, R. J. The Effect of Chemical Oxidation on the Fluorescence of the LH1 (B880) Complex from the Purple Bacterium *Rhodobium marinum*. FEBS Lett. **1998**, 432 (1–2), 27–30.
- (31) Beyer, S. R.; Müller, L.; Southall, J.; Cogdell, R. J.; Ullmann, G. M.; Köhler, J. The Open, the Closed, and the Empty: Time-Resolved Fluorescence Spectroscopy and Computational Analysis of RC-LH1 Complexes from *Rhodopseudomonas palustris. J. Phys. Chem. B* **2015**, 119 (4), 1362–1373.
- (32) Pflock, T.; Dezi, M.; Venturoli, G.; Cogdell, R. J.; Köhler, J.; Oellerich, S. Comparison of the Fluorescence Kinetics of Detergent-Solubilized and Membrane-Reconstituted LH2 Complexes from *Rps. acidophila* and *Rb. sphaeroides. Photosynth. Res.* **2008**, 95 (2–3), 291–298.
- (33) Borisov, A. Y.; Freiberg, A. M.; Godik, V. I.; Rebane, K. K.; Timpmann, K. E. Kinetics of Picosecond Bacteriochlorophyll Luminescence *in vivo* as a Function of the Reaction Center State. *Biochim. Biophys. Acta, Bioenerg.* 1985, 807 (3), 221–229.
- (34) Comayras, F.; Jungas, C.; Lavergne, J. Functional Consequences of the Organization of the Photosynthetic Apparatus in *Rhodobacter sphaeroides*: II. A Study of PufX- Membranes. *J. Biol. Chem.* **2005**, 280 (12), 11214–11223.
- (35) Gerencsér, L.; Laczkó, G.; Maróti, P. Unbinding of Oxidized Cytochrome c from Photosynthetic Reaction Center of Rhodobacter sphaeroides Is the Bottleneck of Fast Turnover. Biochemistry 1999, 38 (51), 16866–16875.
- (36) Sturgis, J. N.; Hunter, C. N.; Niederman, R. A. Spectra and Extinction Coefficients of Near-Infrared Absorption Bands in Membranes of *Rhodobacter sphaeroides* Mutants Lacking Light-Harvesting and Reaction Center Complexes. *Photochem. Photobiol.* 1988, 48 (2), 243–247.
- (37) Ogren, J. I.; Tong, A. L.; Gordon, S. C.; Chenu, A.; Lu, Y.; Blankenship, R. E.; Cao, J.; Schlau-Cohen, G. S. Impact of the Lipid Bilayer on Energy Transfer Kinetics in the Photosynthetic Protein LH2. *Chem. Sci.* **2018**, *9* (12), 3095–3104.
- (38) Liu, L.-N.; Duquesne, K.; Oesterhelt, F.; Sturgis, J. N.; Scheuring, S. Forces Guiding Assembly of Light-Harvesting Complex

- 2 in Native Membranes. Proc. Natl. Acad. Sci. U. S. A. 2011, 108 (23), 9455–9459.
- (39) Cleary, L.; Chen, H.; Chuang, C.; Silbey, R. J.; Cao, J. Optimal Fold Symmetry of LH2 Rings on a Photosynthetic Membrane. *Proc. Natl. Acad. Sci. U. S. A.* **2013**, *110* (21), 8537–8542.
- (40) Chandler, D. E.; Hsin, J.; Harrison, C. B.; Gumbart, J.; Schulten, K. Intrinsic Curvature Properties of Photosynthetic Proteins in Chromatophores. *Biophys. J.* **2008**, 95 (6), 2822–2836.
- (41) Singharoy, A.; Maffeo, C.; Delgado-Magnero, K. H.; Swainsbury, D. J. K.; Sener, M.; Kleinekathöfer, U.; Vant, J. W.; Nguyen, J.; Hitchcock, A.; Isralewitz, B.; et al. Atoms to Phenotypes: Molecular Design Principles of Cellular Energy Metabolism. *Cell* **2019**, *179* (5), 1098–1111.
- (42) Sener, M.; Strümpfer, J.; Timney, J. A.; Freiberg, A.; Hunter, C. N.; Schulten, K. Photosynthetic Vesicle Architecture and Constraints on Efficient Energy Harvesting. *Biophys. J.* **2010**, *99* (1), *67*–75.
- (43) Jang, S. J. Robust and Fragile Quantum Effects in the Transfer Kinetics of Delocalized Excitons between B850 Units of LH2 Complexes. J. Phys. Chem. Lett. 2018, 9 (22), 6576–6583.
- (44) Strümpfer, J.; Schulten, K. Light Harvesting Complex II B850 Excitation Dynamics. J. Chem. Phys. 2009, 131 (22), 225101.
- (45) Baghbanzadeh, S.; Kassal, I. Geometry, Supertransfer, and Optimality in the Light Harvesting of Purple Bacteria. *J. Phys. Chem. Lett.* **2016**, 7 (19), 3804–3811.
- (46) Mascle-Allemand, C.; Lavergne, J.; Bernadac, A.; Sturgis, J. N. Organisation and Function of the *Phaeospirillum molischianum* Photosynthetic Apparatus. *Biochim. Biophys. Acta, Bioenerg.* **2008**, 1777 (12), 1552–1559.
- (47) Milano, F.; Agostiano, A.; Mavelli, F.; Trotta, M. Kinetics of the quinone binding reaction at the Q_B site of reaction centers from the purple bacteria *Rhodobacter sphaeroides* reconstituted in liposomes. *Eur. J. Biochem.* **2003**, 270, 4595–4605.
- (48) Osváth, S.; Maróti, P. Coupling of Cytochrome and Quinone Turnovers in the Photocycle of Reaction Centers from the Photosynthetic Bacterium *Rhodobacter sphaeroides*. *Biophys. J.* **1997**, 73 (2), 972–982.
- (49) Sener, M. K.; Lu, D.; Ritz, T.; Park, S.; Fromme, P.; Schulten, K. Robustness and Optimality of Light Harvesting in Cyanobacterial Photosystem I. *J. Phys. Chem. B* **2002**, *106* (32), 7948–7960.
- (50) Selje, N.; Simon, M.; Brinkhoff, T. A Newly Discovered *Roseobacter* Cluster in Temperate and Polar Oceans. *Nature* **2004**, 427 (6973), 445–448.
- (51) Tang, K.; Zong, R.; Zhang, F.; Xiao, N.; Jiao, N. Characterization of the photosynthetic apparatus and proteome of *Roseobacter denitrificans*. *Curr. Microbiol.* **2010**, *60* (2), 124–133.
- (52) Modern Topics in the Phototrophic Prokaryotes; Hallenbeck, P. C., Ed.; Springer International Publishing: Cham, 2017.
- (53) Scheuring, S.; Gonçalves, R. P.; Prima, V.; Sturgis, J. N. The Photosynthetic Apparatus of *Rhodopseudomonas palustris*: Structures and Organization. *J. Mol. Biol.* **2006**, 358 (1), 83–96.
- (54) Burke, C. M.; Burton, H. R. Photosynthetic Bacteria in Meromictic Lakes and Stratified Fjords of the Vestfold Hills, Antarctica. In *Biology of the Vestfold Hills, Antarctica*; Springer Netherlands: Dordrecht, 1988; pp 13–23.
- (55) El-Sayed, S. Z.; Biggs, D. C.; Holm-Hansen, O. Phytoplankton Standing Crop, Primary Productivity, and near-Surface Nitrogenous Nutrient Fields in the Ross Sea, Antarctica. *Deep-Sea Res., Part A* **1983**, *30* (8), 871–886.
- (56) Crouch, L. I.; Jones, M. R. Cross-Species Investigation of the Functions of the *Rhodobacter* PufX Polypeptide and the Composition of the RC-LH1 Core Complex. *Biochim. Biophys. Acta, Bioenerg.* **2012**, 1817 (2), 336–352.
- (57) Adams, P. G.; Hunter, C. N. Adaptation of intracytoplasmic membranes to altered light intensity in *Rhodobacter sphaeroides*. *Biochim. Biophys. Acta, Bioenerg.* **2012**, *1817* (9), 1616–1627.